

THERMAL REGIME IN THE DIXIE VALLEY GEOTHERMAL SYSTEM

David D. Blackwell¹, Bobbie Golan², and Dick Beniot³

¹Department of Geology, Southern Methodist University, Dallas, TX 75275

²Caithness Corp., 900 N. Heritage Dr., Ridgecrest, CA 93555

³Oxbow Power Services, Inc., 9790 Gateway Dr., Ste 220, Reno, NV 89511

Key Words: Dixie Valley, normal fault, thermal gradient

ABSTRACT

The thermal setting of the Dixie Valley geothermal system is summarized. New data from shallow and deep wells require that the geothermal system be a complex, steeply dipping fault zone with flow on a number of strands of the fault zone rather than a single fault plane. As a result of this new model for the reservoir in Dixie Valley there appear to be numerous untested structures with evidence of fluid flow. The model has applications to other fault controlled, deep circulation systems.

1. INTRODUCTION

The Dixie Valley, Nevada, geothermal field has a rated output of approximately 62 MW and has been producing electrical power for Oxbow Geothermal Corp. since 1988. This field represents the classic Basin and Range fault hosted geothermal system. The thermal source is deep circulation along the Stillwater normal fault zone that bounds the Stillwater Range and Dixie Valley. In 1954 a Ms 6.8 earthquake occurred on the fault zone about 30 km to the south (Bell and Katzner, 1987) so the fault is clearly active. Fluid-entry temperatures in the producing wells range from 220 to 248 °C. The locations of the first exploratory wells were based on land ownership and structure interpretations rather than on gradient exploration data because the rather minimal early thermal gradient studies did not indicate a major anomaly associated with the production area. Shallow gradients are on the order of 100°C/km, not much higher than the regional value in the valley fill of about 55-75°C/km. However, the thermal regime is considerably more complicated and interesting to exploration than realized. The object of this paper is to summarize the shallow and deep thermal data and its relation to the geothermal system.

The Oxbow field has been described by Benoit (1992, 1999). It consists of two groups of production wells in sections 33 and 7 (Figure 1), with injection wells in between (section 5) and to the south (section 18). All deep wells in the Oxbow field had subartesian static water levels when production was initiated. Two hot wells located several km to the southwest, 66-21 (218 °C) and 45-14, (195 °C) have a few lpm of artesian flow. The northernmost well, 76-28 (Tmax of 162 °C at 2350 m) and the 62-21 well in the middle of the valley (Tmax of 184 °C at 3318 m) appear to approach background conditions. The producing zones in the wells are all at about the same depth and the wells are all about the same distance from the range front so that a reservoir model with a single, range bounding, normal fault dipping at about 54° satisfies the observations.

In 1993 and 1994 Caithness Corp. (later joined with ESI to form Dixie Valley Power Partners, DVPP) drilled two deep exploration wells (62A-23 and 36-14) south of the Oxbow field. The reported temperature in 62A-23 is higher than the production temperatures in the Oxbow field (Benoit, 1994). This report represents the first detailed description of the thermal results of that drilling.

Between 1994 and 1998 a number of wells were drilled between the range front and the deep wells. The results clarify the thermal behavior in the area between the deep wells and the various manifestations along the range front. The results from the new deep wells, together with new gravity data, new shallow thermal data, and reinterpretation of the seismic data, result in a new model for the reservoirs in Dixie Valley (Beniot, 1999; Blackwell et al., 1999). This model has applications to other Basin and Range (deep fracture circulation) types of systems.

2. THERMAL DATA SETS

Deep Wells Data from several of the wells in the Oxbow field have become available (see Williams et al., 1997; Wisian et al., 1998). Temperature logs from the 2 wells to the south (45-14 and 66-21), the well to the north (76-28), and the well in the middle of the valley (62-21) are shown in Figure 2. Also shown in Figure 2 is a temperature-depth curve from well 82-5 (a low permeability well between the two groups of producing wells with a Tmax of 226 °C) as an example of reservoir conditions. Wells in section 18, used as injectors, are slightly lower in temperature than in the producing wells in sections 7 and 33. The curves are in equilibrium except for the 66-21 and 45-14 wells which have weak artesian flow (see Williams et al., 1997). The other three curves show essentially conductive conditions with the main effect being the factor of two thermal conductivity contrast between the valley fill and the bedrock and the consequent inverse change in thermal gradient.

In 1993 and 1994 two deep exploration wells (one with two legs) were drilled by DVPP; 62-23, Tmax about 250 °C at 2900 m; 62A-23, Tmax 267 °C at 3475 m TVD; and 36-14, Tmax 280 °C at about 3,050 m TVD. The 62-23 and 62A-23 wells were tight, but the 36-14 well produced from fractures near the bottom of the well and has a shut-in pressure of about 45 bars. The temperature depth curves are shown in Figure 3 for the 62A-23 and 36-14 wells compared to the 82-5 well as a representative of the Oxbow field. The temperatures from 62A-23 were measured in August, 1994, over 8 months after the well was completed. The temperatures shown for 36-14 represent an estimate of the equilibrium curve made from interpretation of a series of nonequilibrium temperature logs made between 7/31/94 and

8/30/94 when the well was at depth between 2600 m (TVD) and about 3050 m (TVD).

Shallow Gradient Drilling In Figure 1 the locations of all of the thermal gradient/heat flow wells are shown. Scattered data were collected before 1994. Eleven 150 m thermal gradient/heat flow holes were drilled in the summer of 1994. These temperature-depth (T-D) curves are shown in Figure 4. Of the 11 holes, 10 were along a line through the Dixie Valley Power Partners (DVPP) lease position in sections 11, 14, 15, and 23 of T24N, R36E (shaded area in Figure 1). The 11th hole (TG#15) was approximately halfway between the 82-5 well and the Senator fumaroles, about 600 m from the front of the Stillwater Range. This well has a deep (below 50 m) gradient of over 200 °C/km and a shallow gradient of over 1,000°C/km. In late 1996 evidence of subsidence (cracks) was noticed in the area east of the Senator fumaroles and in early 1997 steam began to appear from a second set of cracks about 0.6 km SE of the Senator fumaroles. At the same time there was a recognized need for additional injection into the reservoir. Thus during 1997-1998 a number of wells ranging in depth from 60m to almost 400m were drilled between the producing Oxbow wells and the range front. The T-D curves of these wells are described by Allis et al. (1999).

Results The shallow thermal gradients are contoured in Figure 1. The thermal gradient in the valley outside of the geothermal system is between 55 and 75 °C/km. The few gradients in the vicinity of the producing wells in the Oxbow field are 75 to 110 °C/km. The anomalous shallow gradients along the contact of the Stillwater Range and Dixie Valley appear to drop off, possibly to background, to the south of the DVPP lease block and to the north of the Oxbow field. It is unlikely that the decrease in gradients indicates the ends of the geothermal system given the additional thermal manifestations to the north and south along the Stillwater Range/Dixie Valley contact.

Although the data are sparse in places, the contours clearly show two plumes of thermal water leakage from the range front fault into the valley fill. Also shown on Figure 1 are the locations of an area of weak fumaroles along the range bounding fault in sections 10/15 in the DVPP area and a well known area of extensive steam discharge, the Senator fumaroles, near the Oxbow field. The two plumes appear to originate at these fumarole areas along the range/valley contact. Southeast of the Senator fumaroles the shallow gradients are over 2000 °C/km (hatched area on Figure 1) and the temperatures in the wells reach 150°C as shallow as 30 m.

There is local evidence of more recent increase in the temperature in the water table aquifer in some of the wells. For example the temperature-depth curve in TG#5 shows a classic overturn in the temperature-depth curve (see Figure 8 of Ziagos and Blackwell, 1986, curves for 10 to 100 years) due to flow in an aquifer at 14-20 m depth. The time of initiation of the flow is of the order of a few 10's of years so this change might coincide with the 1954 series of

earthquakes, suggesting recent fracturing, at least on a small scale, in the system.

Heat Loss into Valley Fill The excess heat flow associated with the plumes can be used to estimate the heat loss due to the flow of hot water. Based on the thermal gradient anomaly as contoured, the rate of deep geothermal fluid upflow along the approximately 1.5 km of range front in sections 10 and 15 in the DVPP area discharging into the valley aquifer is a minimum of 0.2 kg/s. The wells between the Oxbow field and the Senator fumaroles also have temperature-depth curves showing shallow leakage of very hot water as just described. In this case approximate discharge computes to a value of about 5 kg/s (Allis, 1999).

3. INTERPRETATION OF DVPP DEEP WELL TEMPERATURES

Deep Thermal Results-DVPP Lease The initial exploration model of the geothermal system in the DVPP area (shaded area in Figure 1) was of a single range bounding fault with a dip of about 54°. The drilling of the 62-23 and 62A-23 wells demonstrated that “the range bounding fault” at that location had to dip at an angle of 65° or steeper, however. The 36-14 well basement at only 1 km, only limited geothermal fluid bearing structures near the well above 3,050 m TVD, and increasing temperature to a depth of at least 3,050 m at a point nearly vertically below the topographic edge of the Stillwater Range. Therefore hot water circulating along a single, range bounding, steeply dipping normal fault can not explain the thermal data from the two deep wells.

The constraint on the dip of the thermal structures is that the temperatures continue to increase to depths of at least 3,050 m TVD, and the gradients are essentially constant between 1,200 and 3,050 m (TVD) at 45 °C/km, in 36-14. If the heat source responsible for the high temperatures in 62A-23 had been crossed in 36-14, even if the zone was locally impermeable, the temperatures would become isothermal or decrease with depth. Therefore in 62A-23 the heat source must be below, between, or basinward of the two wells. However, a source below or basinward of the wells is not compatible with the results from 36-14. The heat source responsible for the high temperatures in 36-14 was reached below 3,050 m (TVD), a position that constrains the dip of the fluid bearing structure to be 85 to 90° if it is the range front fault system. Thus the deep well thermal data in the DVPP lease area require at least two major distinct thermal fluid structures to be present.

Two Fault Model A two fault finite difference numerical model was developed based on the temperature and geological constraints from the wells. The geometry inferred for the numerical model is shown in Figure 5. The boundary conditions included a surface temperature of 15°C and an assumed background heat flow of 80 mW/m². Two thermal conductivity values were assumed, one for the Cenozoic units (1.25 W/m/K) and one for the PreCenozoic rocks (2.5 W/m/K). These values are generalized and the factor of two contrast assumed may be locally in error by as

much as $\pm 25\%$. However, the results are not strongly dependent on the exactness of the assumption. Heat transfer is assumed to be conductive except along the fault zone. The circulation of geothermal fluid along the fault controls the assumed temperature at a particular depth. The assumed maximum temperature on the fault zone was $285\text{ }^{\circ}\text{C}$. This temperature is consistent with the results from 36-14. The calculation was done for a period of existence of the system of 70,000 y. That time is long enough to reach near thermal equilibrium over an area on the order of the size of Figure 5. The temperature-depth curves from the deep wells suggest that major transient effects are not generally present and the thermal equilibrium assumption is a good one. The section, shown in Figure 5, is generalized because the strikes of the structures in the area are not constant. Because of the out-of-plane relationships the dips of the faults are also somewhat distorted in places.

Results The exact position of the faults and the temperature distribution on the faults were varied to give a best match for the temperatures in the deep wells. The lateral variation of thermal gradient in the shallow wells is also a constraint on the results of the model. The calculated temperatures along positions corresponding to the tracks of the wells were compared to the observed temperature-depth curves for 36-14 and 62A-23 until a close fit was obtained.

The rounded shape of the temperature-depth curve in 62A-23 is well matched. If the thermal regime in the well were less affected by a nearby steeply dipping heat source, the temperature-depth curve would show more of a kink at the preCenozoic basement. Thus matching the rounded nature of the curve gives a constraint on the distance to the thermal source and the temperatures as a function of depth on the source. The distance of well 62A-23 from the fault is somewhat uncertain because of lack of knowledge of the temperature on the fault zone at its closest approach to the well. It is obviously higher than 267°C and could be as high as $285\pm 5^{\circ}\text{C}$, based on the results from well 36-14. The modeling suggests that the thermal source temperatures are lower than at an equivalent depth along the range front structure, so the temperature is probably between 267 and 275°C (Figure 5). Thus the bottom of well 62A-23 may be within a few hundred meters of a thermal structure.

Except for the gradients in the 600 to 1,200 m range the pattern of temperatures in 36-14 is relatively well matched by the model. One important result of the modeling is that to match the temperatures at 600 to 1,200 m, the valley (piedmont) fault is required to have fluid flow upward to a minimum depth of about 900 m. The shape of the gradient-contours (Figure 1) may also be influenced by flow from this piedmont fault. An attempt to exactly match the temperatures in the 36-14 well in the 600 to 1,200 m depth range is not particularly useful because the extrapolated equilibrium temperature-depth curve has a large associated uncertainty in that depth range.

Some subtleties in the predicted equilibrium temperature-depth curve of 36-14 are matched by the model. The slight possible increase in gradient below 1,800 m as the well

begins to deviate is predicted by some models with a bigger contrast between the temperatures on the two faults. The vertical thermal gradient from the surface to the position of the well bore is an important constraint in the area where there are no surface thermal gradient data. This gradient reflects the integrated magnitude of the thermal gradient and reflects the horizontal variation in temperature gradient as the heat source is approached. The shape of the temperature-depth curve near the bottom of the well is also related to the temperature along the heat source (range bounding fault).

The temperatures in the wells constrain the temperatures on the faults and thus these temperatures are an important result of the modeling. In the case of the range bounding fault zone the temperatures are primarily constrained by the $285\pm 5\text{ }^{\circ}\text{C}$ value at a depth of about 3,050 m (TVD) in 36-14 and the 157°C value at 760 m in an intermediate depth well along the range front (53-15). Because these points intersect the zone almost a 1.5 km apart, it may not be valid to consider them on the same section. However, the presence of high temperatures, and concomitant fluid flow, along the fault for over a kilometer of strike length, is clearly demonstrated. The temperatures at shallow depths on the piedmont fault are constrained by the $150\text{ }^{\circ}\text{C}$ temperatures in the intermediate depth wells and the upper part of 36-14. The deep temperatures there are constrained by the temperatures in 62A-23. This piedmont fault has not been intersected, so its maximum temperature is not known.

In general the temperatures are about $22\pm 11\text{ }^{\circ}\text{C}$ higher on the range bounding structure than on the valley or piedmont one. Temperatures are modeled to be over $230\text{ }^{\circ}\text{C}$ below about 1,800 m along the range front and below about 2,100 m along the basinward thermal source. The temperatures along the piedmont structure are appropriate for those seen in the Oxbow field immediately to the northeast. Thus the region of sections 10, 11, 14 is a source of upwelling fluid that is hotter than the fluid in the Oxbow producing area and so is an area of potential development.

4. DISCUSSION

The thermal data results described in this paper and results of the gravity survey described by Blackwell et al. (1999) give a framework for understanding the structure of the geothermal system in the Dixie Valley area. The general model of the geothermal system is of deep meteoric water circulation and heating in the fractured Basin and Range basement rocks. The fluid flows upward along a complex, active, normal fault zone that bounds the Stillwater Range and Dixie Valley. Above 4,500 m the fault zone includes more than one strand having active geothermal fluid circulation along it (see also Blackwell et al., 1999). The data suggest that there are complex variations of fault structure along the strike of the range/valley contact, and require that it be a series of faults rather than only one structure. For example there are piedmont faults along most of the contact that take up much of the displacement between the range-valley topographic contact and the valley. However, most of the topographic relief is due to a

series of faults within the Stillwater Range (Plank, 1999) and at the range/valley contact that in general have relatively little displacement of the valley fill. Finally the extension process is evident in the ubiquitous occurrence of antithetic faults forming grabens on the hanging wall (down thrown side) of the major faults, a detail not shown on Figure 5 but illustrated in the generalized model of Blackwell et al. (1999). Recent reprocessing of several seismic lines using migration techniques shows that basement underlies the edge of the valley as suggested by the gravity interpretation (DVPP unpublished report, 1994; Honjas in Lettis and Associates, 1998) and delineates several antithetic grabens. The structure of the fault zone deduced here is by no means novel. For example the structure of the fault zone in the area of the 1954 earthquake about 30 km to the south of the Oxbow field shows a range bounding fault zone, a piedmont fault zone, and the antithetic graben system (see Bell and Katzner, 1987).

Some implications of the geometry of the normal fault system for geothermal exploration are clear from examination of Figure 5. For example the fault system along the range front has several targets for drilling, not just one range-front fault. Also the Senator fumaroles may not be updip on the production zone in section 33 since in the model flow on the piedmont faults would be discharged into the valley fill well away from the range. The discharge into the valley fill must happen for the zone feeding the wells in section 7 if there was any natural throughflow before production. Similarly, the fumaroles in sections 15/10 are not updip on the main valley (piedmont) fault because its subcrop intercept at the base of the valley fill is several hundred meters into the valley.

The complexity of the fault zone has an additional attractive feature. The complexity allows for many strands and increases the possibility that one of the strands at any point will be properly oriented to be critically stressed for frictional failure. Hickman et al. (1998) showed that this orientation appears to be the hydraulically conductive orientation.

Deep drilling, temperature gradient exploration, and thermal manifestations together indicate most of these strands have some high temperature fluid flow in some places in the greater Dixie Valley geothermal system. The complexity offers challenges to the exploration and drilling, but it also offers reservoir opportunities and sizes that were not expected based on the single fault model. The lack of temperature inversions in any of the deep wells is consistent with the inference that the reservoir is much larger in volume than a single strand of a Basin and Range normal fault. Thus within the area of these investigations there are a number of potential reservoir structures that have not been tested by drilling. These may already interact with the producing structures via cross faults and/or fracturing, or they may only interact at some unknown depth where all of the strands intersect.

Considerable controversy exists about the overall dip of the Dixie Valley normal fault system. One of the discoveries of

detailed mapping is that there are several steep normal faults parallel to the range front in the area of the Oxbow geothermal field (Plank, 1999). So the evidence seems to point to the range bounding fault being steep (greater than 45°). The strongest evidence for the dip at depth comes from the thermal data. Significant over turns have not been observed below the producing zones in any of the wells (2.5 to 3 km in the Oxbow part of the field). If the structures controlling the geothermal flow were shallow in dip, such overturns might be expected (Wisian, 1999). The position of highest temperatures is not far from the range front and at a depth of about 4 km. Thus there is no doubt the fractures that feed the geothermal field are steeper than 75° within the upper 4 km of the crust (Figure 5).

ACKNOWLEDGMENTS

This work was supported by DVPP and Oxbow Geothermal Corporation. Writing of this paper was supported by USDOE contract DE-FG07971D13504 to SMU.

REFERENCES CITED

- Allis, R. G., S. D. Johnson, G. D. Nash, and D. Benoit, 1999, A model for the shallow thermal regime at Dixie Valley geothermal field, *Trans. Geotherm. Res. Council*, 23, pp. 493-498.
- Bell, J. W., and T. Katzner, 1987, Surficial geology, hydrology, and late Quaternary tectonics of the IXL Canyon area, Nevada, *Nev. Bur. Mines and Geol. Bull.* 102, 52pp.
- Benoit, D., 1992, A case history of injection through 1991 at Dixie Valley, Nevada, *Geothermal Resources Council Trans.*, 16, pp. 611-620.
- Benoit, D., 1994, Review of geothermal power generation projects in the Basin and Range Province, 1993, *Geothermal Res. Council Bull.*, May, 173-178.
- Benoit, D., 1999, A review of various conceptual models of the Dixie Valley, Nevada geothermal field, *Geothermal Resources Council Trans.*, 23, pp. 505-511.
- Blackwell, D. D., D. Benoit, B. Golan, and K. W. Wisian, 1999, Structure of the Dixie Valley geothermal system, a 'typical' Basin and Range geothermal system, *Trans. Geothermal Resources Council*, 23, pp. 525-531.
- Hickman, S. M. Zoback, and R. Benoit, 1998, Tectonic controls on reservoir permeability in the Dixie Valley, Nevada geothermal field, *Proceedings, Twenty-third Workshop on Geothermal Reservoir Engineering*, Stanford University, January 26-28, 6 pp.
- Lettis, W. Associates, Application of advanced seismic reflection imaging techniques to mapping permeable zones at Dixie Valley, Nevada, DOE Final Technical Report, 72 pp., 1998.

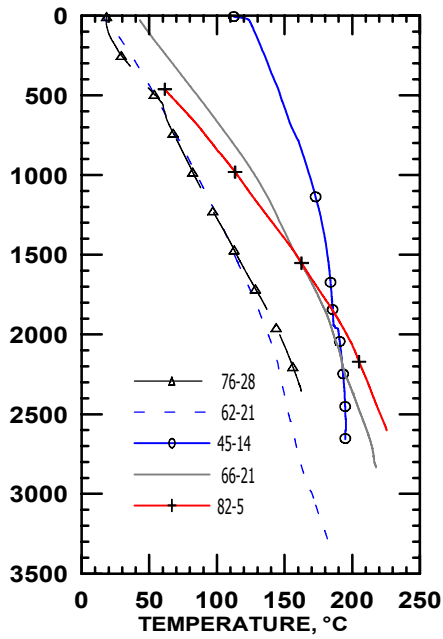


Figure 2. Temperature-depth curves of selected deep wells.

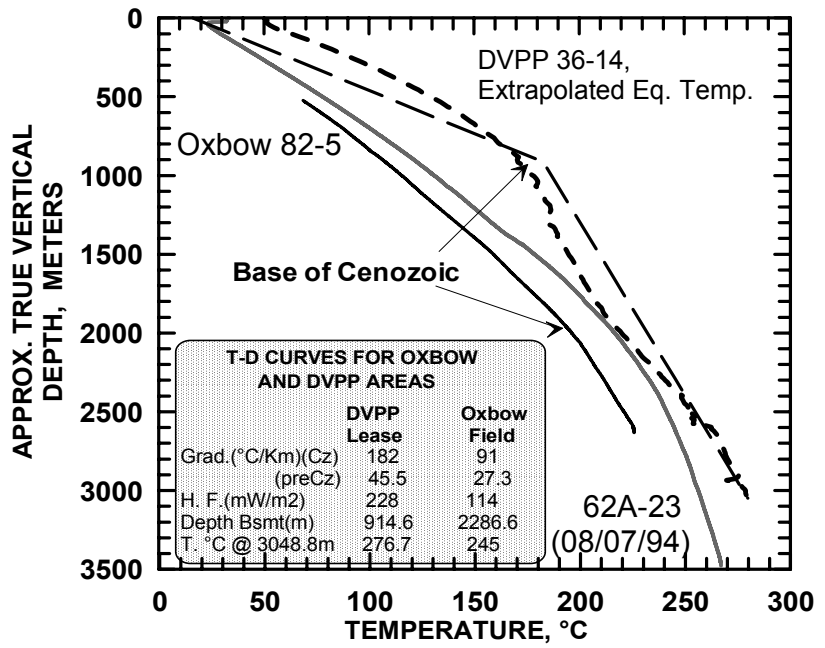


Figure 3. Temperature-depth curves of the 36-14 and 62A-23 wells in the DVPP lease area.

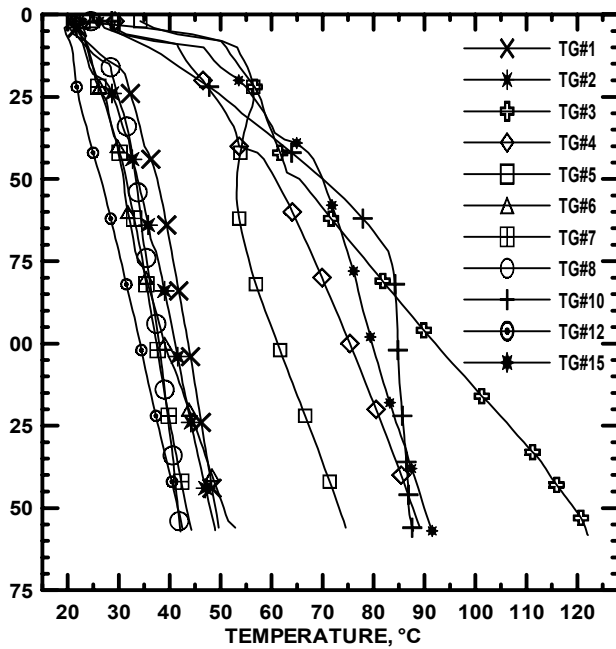


Figure 4. Temperature-depth curves for the Dixie Valley thermal gradient (TG) series of wells in the DVPP lease area. Wells were drilled in the summer of 1994.

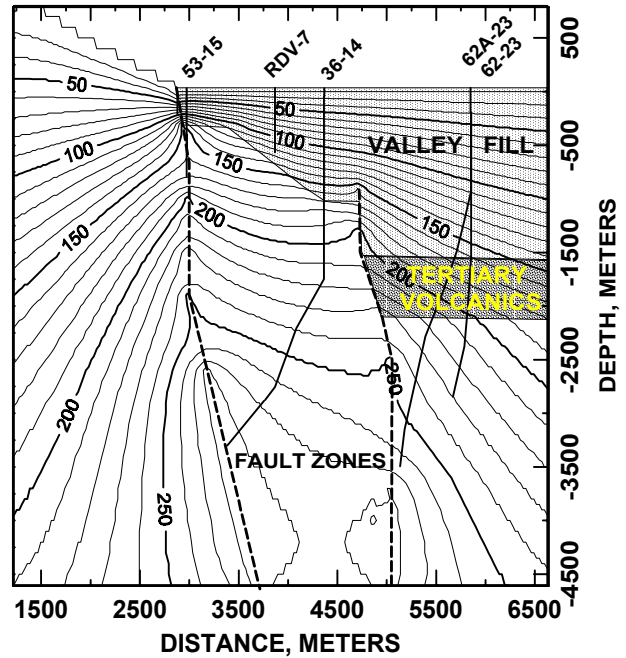


Figure 5. Cross section of part of the Dixie Valley numerical model based on the two fault structural interpretation. Approximate positions and tracks of the 62A-23 (left leg), 62-23, and 36-14 wells are shown. The contours are temperature values and model interpolation from the well logs.